https://doi.org/10.1016/j.precisioneng.2019.07.015

Measurement uncertainty evaluation model in radial composite gear inspection

M. Pueo[1*], R. Acero[2], M.A. Lope[2], J. Santolaria[2]

[1] Centro Universitario de la Defensa. Academia General Militar. Ctra. Huesca s/n. 50090, Zaragoza, Spain

[2] Department of Design and Manufacturing Engineering, University of Zaragoza. María de Luna 3, 50018 Zaragoza, Spain

* Corresponding author. Tel. +34 976739836, fax +34 976739824, E-mail: mpueo@unizar.es

KEYWORDS: Gear metrology; uncertainty; radial composite inspection; double-flank rolling test; worm gear;

A general expression to estimate the measurement uncertainty of double-flank gear rolling tests, according to the uncertainty budget method outlined in the GUM, is presented in this paper. This method is more precise than the comparator method and it allows us to know the individual contributions of each error source. Therefore, it is often applied in secondary calibration laboratories or industrial facilities that require a better understanding of their measurement process capability. Furthermore, the proposed expression can be adapted to estimate the measurement uncertainty of any gear tester configuration that works under rolling principles. The paper describes a case study where the uncertainty budget developed is applied to a double-flank worm gear rolling tester. Using experimental values of calibration and characterization of the gear tester, the expanded uncertainties of the rolling parameters F_i'', F_r'' and f_i'' were calculated. Finally, an optimized uncertainty budget is proposed where the main detected error sources are minimized improving therefore the measurement capacities of the tester.

1. Introduction

Gear rolling tests are the fastest and the most comprehensive way to verify the future gear behaviour in a transmission. Furthermore, they allow detecting manufacturing process errors [1,2]. They are functional gear testing where, in their most common configuration, the gear being inspected (test gear) is rolled against a master gear of better accuracy grade during an entire revolution at low speed. In this manner, the master gear deviations can be considered negligible beside the test gear errors. They are also used to pair off two production gears or to verify the accuracy grade of a complete transmission [3–5].

Despite the fact that this type of testing has been in use for various decades, research interest has increased in the last years because of their metrological potential [6]. Nevertheless, rolling test results can vary from tester to tester even though maintaining the same execution conditions [7–9]. This is because rolling tests are not single measurement of simple geometries but dynamic testing of complex ones. This fact greatly increases the possible error sources, and therefore the difficulty of their evaluation. Nevertheless, the repeatability of gear rolling tests allows considering the measurement process as traceable.

ISO/TC60//WG2 working group engages highly in standardize globally gear parameters but a real unification of gear rolling tests standards to set up parameters, operation conditions and tester's calibration procedures has not been established yet. There are neither accredited laboratories nor national reference rolling patterns that allow us to establish an unequivocal procedure of traceability determining the measurement uncertainty with accuracy. Consequently, the rolling test results are usually only accepted as internal partial validation of the gear's quality, previous agreement between manufacturer and purchaser [6].

In particular, the actual international standards of evaluation of instruments for the measurement of individual gears ISO 18653:2003 [10] and ISO/TR 10064-5:2005 [11] are based on AGMA 931-A2 standard "Calibration of gear measuring instruments (GMIs) and their application to the inspection of product gears" [12], which

grouped all information of the previous AGMA standards. Subsequently, AGMA Calibration Committee decided that similar standardization was needed for the evaluation methods of double-flank rolling testers. Therefore ANSI/AGMA 2116-A05 "Evaluation of double flank testers for radial composite measurement of gears" [13] and AGMA 935-A05 "Recommendations relative to the evaluation of radial composite gear double flank testers" [14] were developed. They provide guidelines on the evaluation and the qualification of this type of machine, as well as the description of some methods for estimating their measurement uncertainty. Annex A of ANSI/AGMA 2116-A05 [13] includes the three common methods for determining uncertainty in the measurement of gears and gear artifacts, extracted from ISO 18653:2003 [10]. Each method differs considerably in complexity, implementation time and cost. Selection is usually determined by the application although their combination is often used in practice.

The surrogate method is generally applied in national and primary calibration facilities. Measurement process is evaluated using non-gear artifacts like eccentric discs or gage blocks. The estimated uncertainty must include the effect of additional factors such as axis alignment, load correction or artifacts geometry which is significantly different to gears. The general form of the uncertainty equation for this method is shown in Equation (*1*), where *U(k)* is the expanded uncertainty; k is the coverage factor; u_m is the standard uncertainty due to reproducibility; u_s is the uncertainty due to calibration artifacts and gauges; $u_{\theta p}$ is the cross-axis alignment uncertainty; u_a is the parallel axis alignment uncertainty; u_L is the load correction uncertainty; u_T is the temperature correction uncertainty.

$$U(k) = k\left[\left(u_m^2 + u_s^2 + u_{\theta p}^2 + u_a^2 + u_L^2 + u_T^2\right)^{0.5}\right] \quad (1)$$

The comparator method is generally used in the gear industry to verify the measuring instrument performance. It evaluates the measurement process using master gears calibrated for different rolling deviations and analysing each parameter separately. In this case, the difference between master gear and test gear must be taken into account [11], what is usually quite complicated [15]. The general form of the uncertainty equation for this method is shown in Equation (*2*), where u_m is the standard uncertainty due to reproducibility; u_n is the master gear calibration uncertainty; u_g is the uncertainty associated with dissimilarity between master gear and test gear geometry; and u_w is the uncertainty associated with differences between master gear and test gear such as material characteristics.

$$U(k) = k\left[\left(u_m^2 + u_n^2 + u_g^2 + u_w^2\right)^{0.5}\right] \quad (2)$$

The uncertainty budget method outlined in the ISO Guide to expression of Uncertainty of Measurement (GUM) [16] is often applied in secondary calibration laboratories or industrial facilities that require a better understanding of their measurement process capability [10,13]. This method is slower and more time-consuming than the comparator method but it is more appropriate for including test gear features. It is usually recommended when the calibration artifact is significantly different to test gear geometry [15,17]. Moreover, it may also be applied to estimate GMIs and CMMs uncertainties. Nevertheless, ANSI/AGMA 2116-A05 [13] does not propose any specific expression or recommendation in order to implement this method.

Uncertainty budget analysis is usually the most suitable approach to analyse the measurement error of double-flank composite inspection. However, few published studies related to uncertainty estimation of double-flank testing could be found [18]. In fact, the developments of new rolling-based gear verification equipment are

practically limited to give repeatability values [19–21] that though validating the test results, do not evaluate the complete measurement process. In addition, there are no publications that show the most influential uncertainty sources in gear rolling measurement process. Their knowledge could lead to reduce measurement uncertainty.

In this work, an expression to estimate double-flank gear rolling test uncertainty, according to uncertainty budget method, is developed. Following the guidelines of ISO GUM [16] and some recommendations of ISO 14253-2 standard [22], the proposed expression allows quantifying individual contribution of each error source in a dynamic measurement. This expression has been used to calculate the measurement uncertainty of a recently upgraded double-flank worm gear rolling tester, using its experimental values of calibration and characterization. In this way, the measurement capability of the tester was evaluated and its improvement points established.

2. Uncertainty budget for double-flank gear rolling test

An uncertainty budget, in accordance with the guidelines of GUM, expresses mathematically the relationship between the measurand and the input quantities that can contribute to the result of the measurement. For that purpose, it is necessary first to determine the estimated value of the input quantity and define its probability distribution; then evaluate the standard uncertainty of each input estimate value and the correlated covariances; after that, determine the combined standard uncertainty of the measurement result; and finally give an expanded uncertainty to provide an interval that may be expected to encompass a large fraction of the distribution of values that could reasonably be attributed to the measurand [16].

As gear measurement involves many error sources that should not be duplicated during the analysis, especially the dominant components. Sometimes this could be avoided and simplified if several error sources are combined by providing the reproducibility values of the measurement process. In this way, most errors due to temperature, assembling and operator could be automatically included. In addition, uncertainty second-order sources could be disregarded. As a general rule, conservative estimates are preferably recommended defining overestimated limits and using rectangular distributions if some data are not known with certainty, provided they are reasonable [17].

2.1 Double-flank gear rolling test description

The double-flank gear rolling test, also known as radial composite test, is the most widespread rolling test due to its simplicity of execution and results' interpretation, although single-flank rolling test can provide more information [23,24]. Test gear is rotated against master gear without backlash at a centre distance lower than the nominal so that two flanks of each gear are simultaneously in contact. For this, an elastic system exerts a constant force on the test gear carriage to be able to measure the variations in the centre distance during an entire revolution (Fig. 1a). The results obtained are presented in a sinusoidal graph (Fig. 1b), where the total radial composite deviation (F_i'') is the difference between the maximum and minimum centre distance within one revolution of the test gear; the tooth-to-tooth radial composite deviation (f_i'') is the greatest difference of the centre distance occurring within an angle of rotation corresponding to the pitch; and the runout by composite test (F_r'') is obtained by the difference between the maximum and minimum value of the long-wave component of F_i''. To determine the accuracy of the test gear, the test values are compared with the reference values, which vary according to their size (diameter and normal module). Although tolerances are set for spur gears they can be used similarly for helical gears. In fact, bevel gears and worm-gear transmissions are usually verified [4,5].

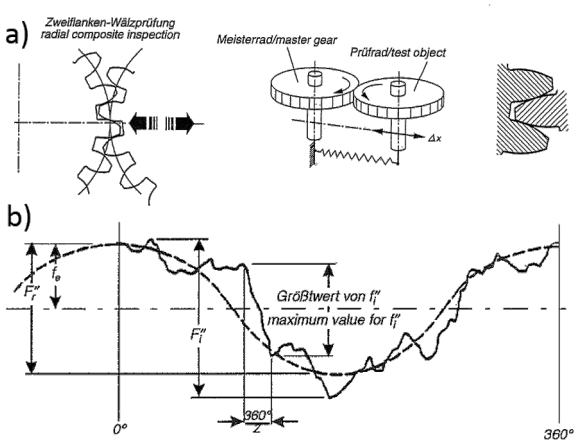

Fig. 1 *Double-flank rolling test (source* [5]*): a) Operating scheme; b) Results interpretation*

2.2 Uncertainty estimation expression

Measurement uncertainty is a parameter that characterizes the dispersion of the values that could reasonably be attributed to the measurand. However, the measurement uncertainty increases with the repeatability of the measurement, but it could also expand due to weak knowledge of relevant test parameters such as device calibration, measuring temperature or the alignment of the instrument. Moreover, the identification of the relevant contributions is usually the most demanding point in a measurement uncertainty estimation [25].

ISO 14253-2 standard [22] divides all possible error components into ten categories (Fig. 2), although a combined effect is usually considered. In particular, ANSI/AGMA 2116-A05 standard [13], recommends to include for double-flank rolling test the following uncertainty contributions: the environmental influence; the artifact and calibration data; the repeatability and reproducibility of the instrument; the runout and mounting error measurement; the mechanical alignment; the probe system filtering, the damping and dynamic response; the servo control system; the evaluation software; and the operator.

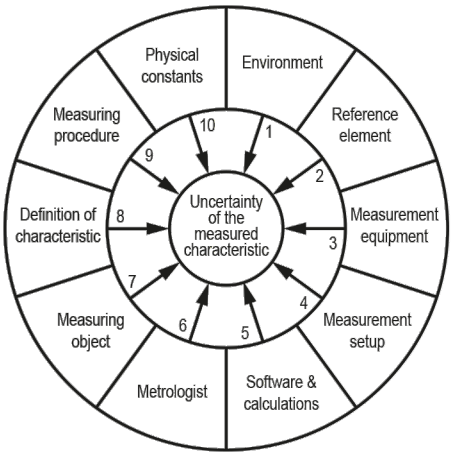

Fig. 2 *Uncertainty components (source [22])*

One way to include all these combined error sources, without the risk of duplicating them, would be to break the rolling parameters (F_i'', F_r'', f_i'') down into the different actions that involve the preparation and execution of double-flank rolling test. The usual measurement process would begin with the initial calibration using gear artifacts or gage blocks to ensure the proper functioning of the tester. The gear axes are then moved to a position

close to the nominal position according to the type and size of the transmission to be verified. After that, the master and test gear are mounted and fixed on the tester. Both gears are now placed with accuracy in their nominal test position and the test gear carriage is released to get the two flanks in contact. Finally, the test is carried out measuring the centre distance between both gears along a complete revolution.

Uncertainty budget for double-flank gear rolling test could be therefore structured according to equation (*3*). It includes the terms of standard uncertainty due to the initial calibration of the equipment (u_0); the displacement from the initial calibration point to nominal test execution position (u_{dis}); the mounting and clamping of the gears (u_{gear}); and finally the effects of double-flank rolling test execution (u_{df}). However, if we want to obtain a valid estimated value of uncertainty it is necessary to decompose each of the uncertainty terms in their most elementary components. In this way, individual effects can be determined from experimental values of the tester calibration and characterization. Particularly, each uncertainty term is described in detail in Subsection 3.4.

$$U(k) = k\left[\left(u_0^2 + u_{dis}^2 + u_{gear}^2 + u_{df}^2\right)^{0.5}\right] \qquad (3)$$

3. Case study

A worm gear rolling tester has been developed, from an obsolete gear profile measuring machine, integrating double-flank and single-flank rolling tests on a single machine. This tester configuration, so rare in commercial rolling equipment, allows characterizing potential error sources, maintaining identical execution conditions in both tests [26]. The general indications of VDI/VDE 2608 [5], AGMA 915-1-A02 [27] and AGMA 915-2-A05 standards [28], as well as the guidelines of ANSI/AGMA 2111-A98 standard [29], have been followed for its development. The latter is the only standard that schematically describes rolling tests for worm gear transmission (Fig. 3). In particular, this work focuses on establishing the measurement uncertainty values of double-flank rolling parameters applying equation (3) to the tester in study. Figure 3b shows the most common arrangement of master worm and test worm gear in this type of testing, as well as the measurement direction.

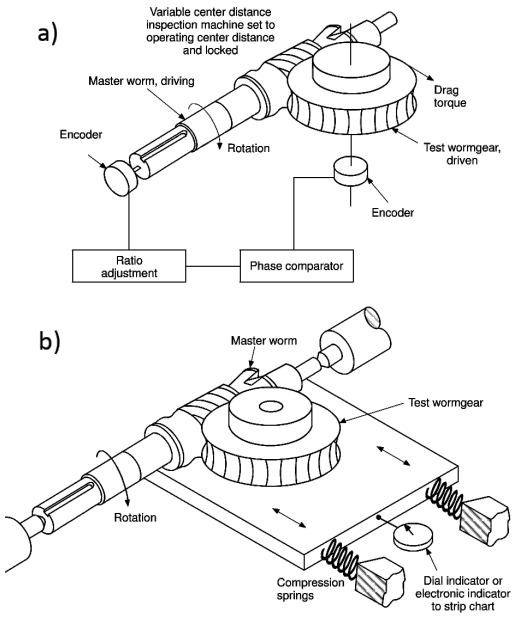

Fig. 3 *Schematic of worm gear testers (source* [29]*): a) Single-flank test; b) Double-flank test*

3.1 Tester description

The gear-rolling tester is able to verify worm gears of up to 600 mm diameter until accuracy grade 6 using master worms of up to 150 mm diameter and 1000 mm long. It has a classical structure that could be divided in three principal parts: bed plate (1 in Fig. 4), worm holder column (2 in Fig. 4) and worm gear holder carriage (3 in Fig. 4).

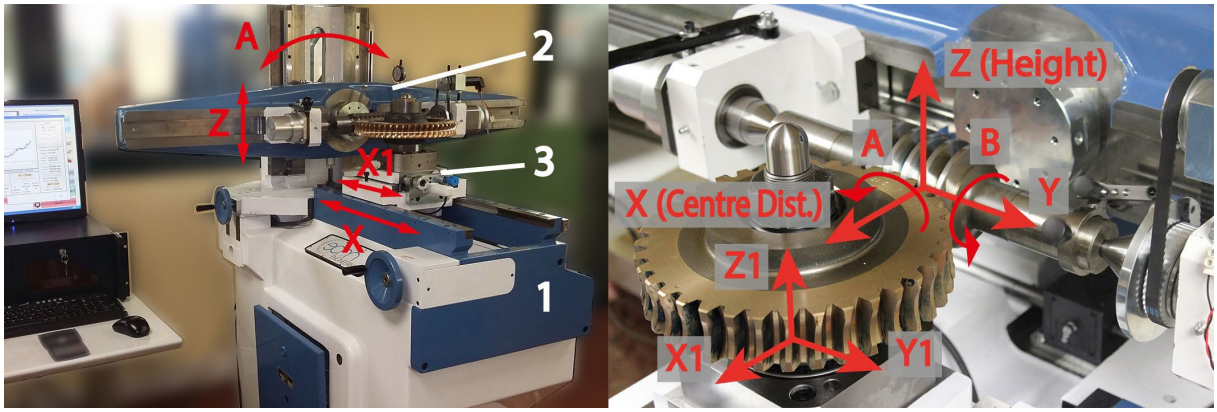

Fig. 4 *Worm gear rolling tester*

The worm holder column is located on one side of the cast steel bedplate where master worm is mounted between centres (Fig. 4). The column incorporates a carriage that allows vertical movement of the master gear to the nominal test height (Z-axis), by means of a handwheel. Its position is monitored by a linear encoder fixed to the column (Table 1). Additionally, the crosspiece allows adjusting the perpendicularity between the axis of master worm (Y-axis) and the axis of the worm gear (Z1-axis). A dial gauge is used to establish the angle variation between them measuring the height difference of a point at a known fixed distance with regard to crosspiece rotation axis (A-axis). On the other side, the worm gear holder carriage, where worm gear is clamped, slides horizontally to place the worm gear at the nominal centre distance (X-axis). Its position is also monitored by another linear encoder fixed to the bed plate (Table 1). Over this principal carriage, a second horizontal carriage is unlocked to perform the characteristic back and forth movement of double-flank rolling tests (X1-axis). This continuous displacement is measured by a length gauge (Table 1) and provides the rolling values. Moreover, the tester includes an angular encoder aligned with the axis of the master worm (Y-axis) that determines the rotated angle at each point of measurement. Table 1 shows the characteristics of the different movements of the tests as well as the measuring instruments of the machine to control them.

Table 1 *Summary of the measuring instruments and tester characteristics*

Characteristics	Axis	Max. values	Measuring instrument	Accuracy
Centre distance displacement	X-axis	400 mm	Linear encoder Heidenhain LF481C	± 3 µm
Height displacement	Z-axis	120 mm	Linear encoder Heidenhain LF481C	± 3 µm
Double-flank test measurement	X1-axis	5 mm	Length gauge Heidenhain ST 1288	± 1 µm
Worm axis angle variation	A-axis	± 3º	Dial gauge TESA	± 1 µm
Worm rotation angle	B-axis	360º	Angle encoder Heidenhain RON285C	± 2.5 arcsec
Worm rotation speed	A-axis	30 rpm	-	-
Elastic system force	X1-axis	100 N	-	-

3.2 Calibration and testing conditions

The tester considered in this work is located in the metrological laboratory of a gear manufacturer. Both the calibration of the equipment and the characterization tests of this study were carried out under stable conditions of cleanliness and temperature (20º ± 0.5º) over several weeks.

The few recommendations for calibration and verification described for rolling testers [13,14] as well as for general gear measuring equipment [10,11], were followed as far as possible. In addition, it was necessary to apply techniques commonly used in the calibration and verification of machine tools, MMCs and GMIs [30–34]. Axes arrangement in worm transmissions limits the use of the most common standard artifacts.

Table 2 shows the main characteristics of the master worm and the product worm gear that were used in the tests. Flank tolerance class of the master worm was established as grade 3 by means of individual profile, helix and pitch measurements, according to ISO 1328-1:2013 [3]. Nominal test position was at a centre distance of 170 mm and at a height of 45 mm between the hobbing plane and the reference surface of the worm gear. Due to its dimensions and characteristics, this transmission could be considered as a representative transmission in lifting and solar industry. Tests were carried out at a constant rotational speed of the worm of 25 rpm, always in the same direction. The elastic system was regulated with a pushing force of 85 N. Moreover, the same initial point (same tooth) was used at the beginning of each test to ensure measurements on the same tread.

Table 2 *Geometrical characteristics of the gears*

Master worm reference diameter	59 mm
Master worm teeth number	1
Worm gear reference diameter	281 mm
Worm gear teeth number	55
Normal module	5.09 mm
Pressure angle	20
Helix Angle	4.949º

On the other hand, Table 3 shows the reference values of double-flank rolling parameters to establish ISO accuracy grades [3,4] depending on the gear size to be verified. Accuracy grade is determined by the worst accuracy grade of any of its rolling parameters. All measured values must be lower than the established reference values to consider a gear within an accuracy grade. A few microns determine the leap from one grade to another, showing this fact the need of establishing the measurement uncertainty as accurately as possible, especially for the highest accuracy grades. Nevertheless, uncertainties of up to 30% are accepted in gears verification with values to be evaluated below 10 microns [13].

Table 3 *Double-flank parameters values for 281 mm reference diameter and 5.09 mm normal module according to ISO accuracy grades [3,4].*

Grade	F_i'' (µm)	F_r'' (µm)	f_i'' (µm)
4	30	16	11
5	42	23	15
6	60	32	22
7	84	45	31
8	119	64	44

3.3 Sources of error

Error propagation models are usually unknown in gear metrology. Considering only the calibration of gear measuring machines, there are many error sources that combine themselves in a different manner for each gear geometry. Therefore, an alternative is to quantify the sources of error, compensate them, if possible, and finally consider their effects in the uncertainty budget [32]. In this work, we consider as error sources of the radial composite test every factor generating an error in the readings of the tester measuring instruments and therefore influencing the result of the measurement. The possible differences with the real values must be included as terms in the uncertainty budget. Some errors are intrinsic to the measuring instruments themselves, meanwhile others can be extracted from the calibration procedure, the initial verification or the test execution.

3.3.1 Calibration procedure errors

Laser interferometry and gravity-based methods are common techniques used for geometric errors measurement and compensation of machines [30]. To calibrate the rolling gear tester we used a Renishaw XL-80 laser interferometer and an electronic level Fowler Wyler Minilevel 54-810-200 (Fig. 5). The interferometer provided a linear accuracy of 0.5 ppm and angular accuracy of ± 1 μm / m; and the electronic level an accuracy of 2 %.

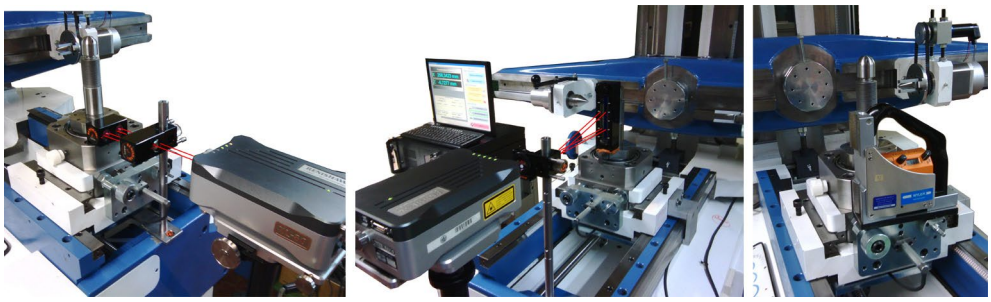

Fig. 5 *Tester calibration set up*

First, numerical compensations of the linear encoders and the length gauge were applied in the machine software to minimize the misalignments between them and the carriages' movements. For that, we compared the measurement instruments and the interferometer readings in different positions for a complete traverse of the moving components.

Five bi-directional approaches [34] were carried out with the following positions: (i) each 5 mm for the linear encoder measuring the height displacement (Z-axis); (ii) each 10 mm (from 0 to 200 mm) and 25 mm (from 200 to 400 mm) for the linear encoder measuring the center distance displacement (X-axis); and (iii) each 0,05 mm (from 0 to 0.3 mm) and 0,5 mm (from 0.3 to 5 mm) for the length gauge quantifying the double-flank test displacement (X1-axis). With the data obtained, we applied a least square compensation polynomial function that minimized the positioning error. After applying the function, the linear positioning errors of each measurement instrument were obtained (E_{ZZ}, E_{XX}, E_{XX1} in Table 4) by means of the difference between the maximum and minimum value of the compensated positions (see Fig. 6). These residual values were included as errors sources in the uncertainty budget.

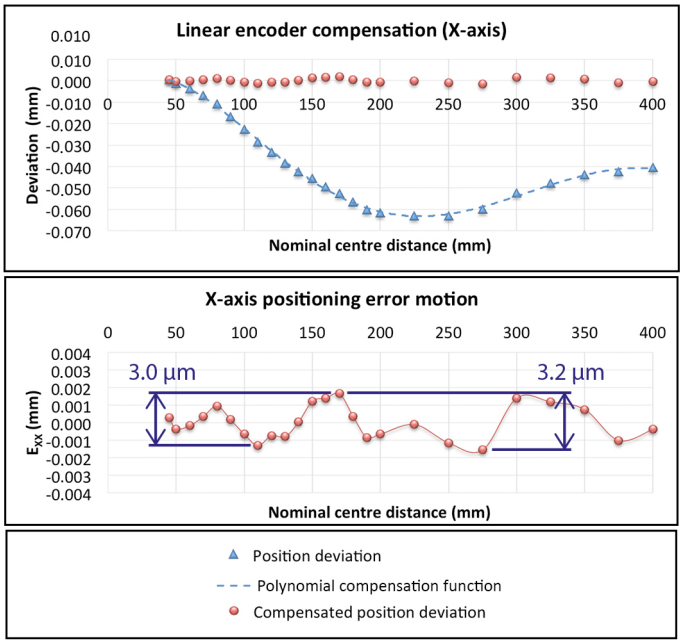

Fig. 6 *Linear encoder numerical compensation and main carriage positioning error (X-axis)*

In addition, we estimated the remaining geometric errors of the carriages displacements with the same procedure using five bi-directional approaches with identical positions for each axis and error. The straightness errors were calculated as the value of the largest positive straightness deviation added to the absolute value of the largest negative straightness deviation with respect to the least squares reference straight line. The angular errors were calculated as the value of the largest positive angular deviation added to the absolute value of the largest negative angular deviation, evaluated in each one of the three orthogonal directions [33].

Some of these errors could modify the testing results without being perceptible by the measuring instruments. For example, the relative height between the gears could change if the main carriage moves along the x-axis due to the vertical straightness (E_{ZX}) and the pitch errors (E_{BX}). Besides, the roll error (E_{AX}) could affect the axis perpendicularity in the same displacement along the X-axis. Nevertheless, other geometric errors are negligible such as the ones derived from the secondary axis (X1-axis) movement due to its small travel. Others have directly no effect on the results like the x-axis straightness error motion in the y-axis direction (E_{YX}) because of the single moving of the meshing point. Table 4 shows the unwanted deviations in the motions of the axis at the meshing point between master gear and test gear. They are the error values at the functional point used to estimate the measurement uncertainty considering the lenses' position and the maximum size of the worm gear test. They are grouped according to the parameter that modifies in the testing (see first column): centre distance, height or perpendicularity. This links directly to the sensitivity coefficients explained in 3.3.4 subsection. It is important to highlight that despite we defined the errors according to ISO 230-1:2012 [33], the pitch error motion values (E_{BX} and E_{BZ}) are expressed as a distance magnitude and not angular one, representing the maximum vertical deviation of the mesh point, which is calculated considering the maximum angular deviation. In this way, we could link the pitch errors with the uncertainty of the rolling parameters through the sensitivity coefficients. On the other hand, the fourth column shows the errors of the maximum carriages displacements, while the last column includes the errors considering carriage displacements reduction to the most usual working area of the tester. We included a limitation in the worm gear diameter of 400 mm and a displacement up to 200 mm for the X-axis and up to 50 mm

for the Z-axis. This allows achieving a more realistic measurement uncertainty estimation because this type of tester usually works for ranges of measurement smaller than its maximum capacity.

Table 4 *Geometric errors at the meshing point due to carriages displacements*

Affected parameter	Error	Description	Total volume	Reduced working area
Centre distance	E_{XX}	X-axis linear positioning error	3.2 µm	3.0 µm
	E_{XX1}	X1-axis linear positioning error	0.4 µm	0.2 µm
Height	E_{ZZ}	Z-axis linear positioning error	4.3 µm	2.3 µm
	E_{ZX}	X-axis straightness error in Z-axis	56 µm	17 µm
	E_{BX}	X-axis error around B-axis	76 µm	43 µm
	E_{BZ}	Z-axis error around B-axis	9 µm	2.1 µm
Perpendicularity	E_{AX}	X-axis angular error around A-axis	13 arcsec	10 arcsec
	E_{AZ}	Z-axis angular error around A-axis	28 arcsec	5 arcsec

3.3.2 Errors due to tester starting and initial calibration

Tester starting has also some measurement uncertainty associated. First, the perpendicularity between rotation axes of the gears must be checked. For this purpose, it is verified that two points, one on each side of a calibrated cylindrical gauge placed in the position of the worm, are at the same height when a dial gauge is rotated on the worm gear holder shaft [35] (Fig. 7a). Then, the cylindrical gauge and the worm gear shaft are brought into contact. Both cylinders were measured with a Zeiss WMM-850 CMM whose expanded uncertainty is U_{99} (k = 3) = 1µm for a small calibrated range of measuring. Knowing exactly their diameters (d_{cgw}= 54,796 mm and d_{cgwg}= 34,995 mm) allows us to calibrate the readings of the centre distance and the relative height between the gears (Fig. 7b). Moreover, all instruments, elements and movements involved were considered in the uncertainty budget, such as the repeatability in the blocking of the secondary carriage (S_{rsc} = 0.4µm) or the hysteresis of the perpendicularity regulation system (H_{pr} = 2.95 arcsecs). In both cases, we made a series of ten repetitions where the nominal positions (centre distance and relative height between the gears) were modified and then restored including any error sources in the repeatability values.

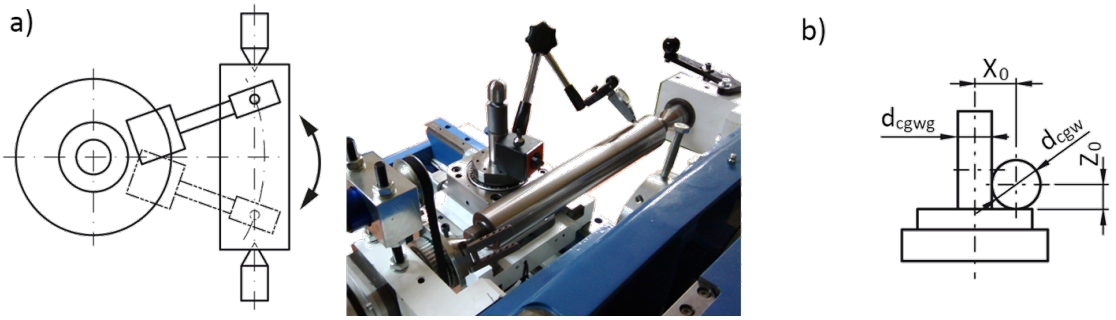

Fig. 7 *Initial calibration: a) Perpendicularity verification; b) Centre distance and height calibration by direct contact*

3.3.3 Testing execution errors

The mounting and clamping of the master worm and worm gear for the execution of tests are also sources of uncertainty. Furthermore, gears' manipulation by the operator always implies a certain range of variation. Repeatability data were extracted from five repetition series of ten tests in which the worm, or the worm gear

when applicable, was disassembled and then mounted in its position again to re-run the test while maintaining the remaining operating conditions. These series represent the random assembling of the gears in any possible position. Therefore, the repeatability values also include the small geometric errors that the master worm contributes on measurement uncertainty, even though they are usually negligible compared with the worm gear deviations when, according to VDI/VDE 2608:2001 [5], there is a difference of more than three accuracy grades. Table 5 shows the range of variation of the worm and worm gear obtained for the rolling parameters.

Table 5 *Worm and worm gear repeatability*

	F_i'' (μm)	F_r'' (μm)	f_i'' (μm)
Worm error variation range (E_{worm})	0.9	0.5	1.1
Worm gear error variation range (E_{wgear})	10.2	9.8	1.6

Likewise, it was experimentally determined that there was hardly any variation in the results of the rolling tests when the execution speed and/or the elastic system force were modified, as long as they were within the established limits by VDI 2608 standard [5] (below 30 rpm and 100 N). Nevertheless, this circumstance might come from filter and damping effects. Therefore, although in this case they were considered as negligible in the uncertainty budget, this statement could not be applicable to all gear sizes, transmissions and rolling testers. On the other hand, the measurement data density was of 8192 points (2^{13} points) per revolution, that is to say 148 points per tooth. This data density, five times more than the recommended minimum number of measurement points to evaluate rolling parameter [3], prevents any aliasing effect or noise. Moreover, the cut-off frequency to filter long and short wavelength components was established at 33%.

3.3.4 Sensitivity coefficients

Partial derivatives that describe how the output estimate varies according to variations in the values of the input estimates are referred to as sensitivity coefficients. They can be experimentally determined, instead of calculating them from a function, measuring the output variation produced by the variation of a given input magnitude, maintaining the remaining input quantities constant [16].

The results of double-flank rolling tests do not come from a direct unitary measurement but from a more complex process. Therefore, the errors in the centre distance; in the relative height between hobbing planes; and in the perpendicularity between gears' axes do not affect to rolling parameters equally. Each error source has different impact on the measurement uncertainty and this is reflected by the sensitivity coefficients on each term. In particular, the experimental characterization of the tests allowed establishing their values. Three test repetition series were performed for that purpose where the centre distance (cd), the height (h) or the perpendicularity between axes (p) was varied gradually, while maintaining the rest of conditions. Testing results in different positions were obtained for each series, above and below the nominal position. Repetitions in 7 positions every 50 μm were carried out to establish the centre distance (c_{cd}) and height (c_h) sensitivity coefficients. Repetitions in 15 positions every 37 arcsec (50 μm in dial gauge) were carried out to establish the axes perpendicularity sensitivity coefficient (c_p). Finally, the ratio between the maximum variations of each rolling parameter (F_i'', F_r'', f_i'') and their nominal positions' variations determined the sensitivity coefficients of each series (cd, h, p). Table 6 shows the experimental sensitivity coefficients values that must be applied to each rolling parameter in the uncertainty budget.

Table 6 *Experimental sensitivity coefficients*

Sensitivity coefficients	Units	F_i''	F_r''	f_i''
Centre distance (c_{cd})	µm/µm	0.013	0.022	0.019
Height (c_h)	µm/µm	0.040	0.013	0.032
Perpendicularity (c_p)	µm/arcsec	0.039	0.037	0.021

3.4 Breakdown of uncertainty budget of F_i''

The main parameter measured in double-flank test, F_i'', comes from the difference between the maximum and the minimum centre distance when the gears are rolled without play during a complete revolution (equation *4*) where $a''_{measurement}$ is the measured centre distance; and $a''_{theoretical}$ is the theoretical design centre distance when left and right-hand flanks of the gears remain meshed at the same time. Moreover, measurement error (Error) is considered as the difference between the instrument readings ($a''_{measurement}$) and the actual centre positions (a''_{real}) between master worm and worm gear (equation *5*). The uncertainty budget allows determining the probable error range.

$$F_i'' = Max\left(a''_{measurement} - a''_{theoretical}\right) - Min\left(a''_{measurement} - a''_{theoretical}\right) \quad (4)$$

$$Error = a''_{measurement} - a''_{real} \quad (5)$$

In this subsection, the terms of the proposed general expression (equation 3) are broken down into their elementary error components. A combined standard uncertainty value (u_c) of the measurement process, and therefore an expanded uncertainty value (U_{95}) with coverage factor k=2, can be estimated applying the errors of the measuring instruments (Table 1), the calibration and characterization values (Table 4, Table 5), as well as the sensitivity coefficients (Table 6). In general, we defined conservative uncertainty estimations. The components of the measurement uncertainty model were evaluated through Type A or Type B evaluations. For example, Type A was considered for the evaluation of the measurement uncertainty in the blocking of the secondary carriage and the measurement of the cylindrical gauge and the worm gear shaft. It was characterized by the standard deviations of the measurements (subsection 3.3.2). On the other side, for the uncertainty estimation of the measurement instruments, we selected Type B evaluations following a rectangular distribution function with a limit value (a) corresponding to the accuracy of the verified measuring instrument (Table 1). In the case of the geometric errors due to carriages displacements, we used a type B evaluation with a rectangular probability function with a limit value (a) corresponding to the half of the geometric errors shown in Table 4. Identical evaluations were used for assessing the uncertainty derived from the repeatability in the perpendicularity regulation system and the effect on the temperature variation in the measurement of the cylindrical gauge and the worm gear shaft (subsection 3.3.2). Finally, the experimental data showed that the gears assembling repeatability could be better characterized with a type B evaluation according to a symmetric Gaussian probability function with limit value (a) equal to the half of the variation ranges obtained (Table 5).

3.4.1 Initial calibration uncertainty (u_0)

This uncertainty term must include all those possible errors derived from the initial calibration and the gear artifacts used. In this case, a calibrated cylindrical gauge in the worm position and the worm gear shaft, whose diameters are known, are brought into contact. This action validates the linear probe and the linear encoders readings in the centre distance and height measurement, but assuming uncertainty. The calculation of the

uncertainty due to initial calibration of the equipment, including the different error components and their associated sensitivity coefficients, is shown in equations (*6*) and (*7*) where the law of error propagation has been applied.

$$u_0^2 = u_{0cg}^2 + u_{0encx}^2 + u_{0lgx1}^2 + u_{0cgz}^2 + u_{0encz}^2 + u_{0p}^2 = \left[\left(\frac{1}{2}\right)^2 u_{0cgw}^2 + \left(\frac{1}{2}\right)^2 u_{0cgwg}^2\right] + u_{0encx}^2 + \left(u_{lgx1}^2 + u_{rsc}^2\right) + u_{0cgz}^2 + u_{0encz}^2 + \left(u_{pr}^2 + u_{pdg}^2\right) \quad (6)$$

$$u_0^2 = \left(\frac{1}{2}\right)^2 c_{cdFi}^2 \left\{\left[\left(\frac{U_{99\,(CMM)}}{k_{CMM}}\right)^2 + \frac{{s_{cgw}}^2}{n} + \left(\frac{d_{cgw}\alpha_{max}\Delta t_{max}}{\sqrt{3}}\right)^2\right] + \left[\left(\frac{U_{99\,(CMM)}}{k_{CMM}}\right)^2 + \frac{{s_{cgwg}}^2}{n} + \left(\frac{d_{cgwg}\alpha_{max}\Delta t_{max}}{\sqrt{3}}\right)^2\right]\right\} + c_{cdFi}^2\left(\frac{E_{encx}}{\sqrt{3}}\right)^2 + c_{cdFi}^2\left(\left(\frac{E_{lgx1}}{\sqrt{3}}\right)^2 + \frac{s_{rsc}^2}{n}\right) + \left(\frac{1}{2}\right)^2 c_{hFi}^2\left[\left(\frac{U_{99\,(CMM)}}{k_{CMM}}\right)^2 + \frac{{s_{cgw}}^2}{n} + \left(\frac{d_{cgw}\alpha_{max}\Delta t_{max}}{\sqrt{3}}\right)^2\right] + c_{hFi}^2\left(\frac{E_{encz}}{\sqrt{3}}\right)^2 + c_{pFi}^2\left[\left(\frac{H_{pr}/2}{\sqrt{3}}\right)^2 + \left(\frac{E_{pdg}}{\sqrt{3}}\right)^2\right] \quad (7)$$

The first term (u_{0cg}) is the uncertainty associated with the errors of the calibrated cylinders used. It has been divided into the uncertainty due to the measurement of the cylindrical gauge (u_{0cgw}) and the measurement of the worm gear shaft (u_{0cgwg}). In both cases, the uncertainty of the CMM used (subsection 3.3.2), the standard deviations of the measurements (S_{cgw}= 0.2 µm, S_{cgwg}= 0.3 µm, n=10 observations) and the possible variations of the diameters due to the laboratory temperature oscillation during their measurement (α_{max}= 1.25·10^{-5} °C^{-1}, Δt_{max}= 0.5°C) were considered. Moreover, c_{cdFi} coefficient of sensitivity has been applied because the uncertainty of the rolling parameters can only affect the centre distance.

The second term is the uncertainty due to the error of the linear encoder that verifies the principal carriage positions (u_{0encx}). It only includes the uncertainty derived from the instrument error, linear encoder in the x-axis (E_{encx}). The third term is the uncertainty associated with the length gauge that measures the secondary carriage positions (u_{0lgx1}). It is composed of the uncertainty due to the instrument error (u_{lgx1}), which is calculated from its accuracy error (E_{lgx1}); and the uncertainty due to the repeatability in the secondary carriage locking (u_{rsc}), calculated from its standard deviation (S_{rsc}). c_{cdFi} coefficient of sensitivity has also been applied in this terms.

The fourth term is the uncertainty associated with the cylindrical gauge used in the height calibration (u_{0cgz}) and the fifth term is the uncertainty due to the error of the z-axis linear encoder (E_{encz}) that controls the vertical carriage displacements (u_{0encz}). These terms are very similar to the first and second ones although a different coefficient of sensitivity has to be applied (c_{hFi}) because they generate errors in height variation.

The last term is the uncertainty due to the calibration of the perpendicularity between the gears' axes (u_{0p}). It has been divided into the uncertainty due to the error of the regulation itself (u_{pr}), which is calculated from the hysteresis of the system (H_{pr}); and the uncertainty of the dial gauge used (u_{pdg}), calculated from its accuracy error in angular value (E_{pdg}). In this case, c_{pFi} coefficient of sensitivity has been applied.

3.4.2 Uncertainty of the displacement to the nominal test position (u_{dis})

The displacements of the worm gear holder carriage (main horizontal carriage) and worm carriage (vertical) from the calibration point to their nominal test positions have to be considered as uncertainty terms (u_{cd} and u_h

respectively). Equation (*8*) shows how the different components of the uncertainty associated with both movements have been divided. The uncertainties due to the accuracy of the laser interferometer used for the calibration (u_{ilx} and u_{ilz}) and the errors of linear encoders are included (u_{encx} and u_{encz}), as well as, the uncertainties due to the backlash of the mechanical systems (u_{cdb} and u_{hb}). They have been broken down into uncertainties due to the residual compensation values of the measurement instruments (u_{cdc} and u_{hc}) and the geometrical errors' components (u_{cdEZX}, u_{cdEBX}, u_{cdEAX}, u_{hEBZ}, u_{hEAZ} and u_{hEXZ}). Equation (*9*) shows the breakdown of each term into the elementary form. This allows estimating the measurement uncertainty from the tester calibration values. In particular, the sensitivity coefficient to be applied depends on how each error influences the rolling parameters.

$$\begin{aligned} u_{dis}^2 = u_{cd}^2 + u_h^2 &= \left(u_{lix}^2 + u_{encx}^2 + u_{cdb}^2\right) + \left(u_{liz}^2 + u_{encz}^2 + u_{hb}^2\right) \\ &= \left[u_{lix}^2 + u_{encx}^2 + \left(u_{cdc}^2 + u_{cdEZX}^2 + u_{cdEBX}^2 + u_{cdEAX}^2\right)\right] \\ &+ \left[u_{liz}^2 + u_{encz}^2 + \left(u_{hc}^2 + u_{hEBZ}^2 + u_{hEAZ}^2 + u_{hEXZ}^2\right)\right] \end{aligned} \tag{8}$$

$$\begin{aligned} u_{dis}^2 = &\left\{c_{cdFi}^2\left(\frac{E_{lix}}{\sqrt{3}}\right)^2 + c_{cdFi}^2\left(\frac{E_{encx}}{\sqrt{3}}\right)^2\right. \\ &\left. + \left[c_{cdFi}^2\left(\frac{E_{XX}/2}{\sqrt{3}}\right)^2 + c_{hFi}^2\left(\frac{E_{ZX}/2}{\sqrt{3}}\right)^2 + c_{hFi}^2\left(\frac{E_{BX}/2}{\sqrt{3}}\right)^2 + c_{pFi}^2\left(\frac{E_{AX}/2}{\sqrt{3}}\right)^2\right]\right\} \\ &+ \left\{c_{hFi}^2\left(\frac{E_{ilz}}{\sqrt{3}}\right)^2 + c_{hFi}^2\left(\frac{E_{encz}}{\sqrt{3}}\right)^2\right. \\ &\left. + \left[c_{hFi}^2\left(\frac{E_{ZZ}/2}{\sqrt{3}}\right)^2 + c_{hFi}^2\left(\frac{E_{BZ}/2}{\sqrt{3}}\right)^2 + c_{pFi}^2\left(\frac{E_{AZ}/2}{\sqrt{3}}\right)^2 + c_{cdFi}^2\left(\frac{E_{XZ}/2}{\sqrt{3}}\right)^2\right]\right\} \end{aligned} \tag{9}$$

3.4.3 Gears assembling uncertainty (u_{gear})

The influence of the handling, mounting and clamping of the gears, as well as the calibration of master worm, on the rolling parameters must be included in terms of uncertainty. Small misalignments between rotation axes, the backlashes in the assembling or the way of working of the operator generate mainly eccentricities that are difficult to quantify at individual level. Moreover, small geometric errors effects of master worm were considered into this uncertainty component. For this reason, uncertainty definition of master worm (u_{worm}) and worm gear to be verified (u_{wgear}) has been determined experimentally from the repeatability of its behaviour as it was stated in section 3.3.3. In this case, it is established the limit error of a symmetric Gaussian probability distribution (E_{worm} and E_{wgear}). In addition, the uncertainty term of the calibration of the master worm (u_{worm0}) has been included, although usually the influence of the master gear can be considered negligible compared with the test worm gear deviations [5]. In this way, the uncertainty calculation is carried out according to equation (*10*). Moreover, a sensitivity coefficient equal to 1 has been applied because repeatability values are direct values of uncertainty of the rolling parameters.

$$u_{gear}^2 = u_{worm}^2 + u_{worm0}^2 + u_{wgear}^2 = \left(\frac{E_{worm}/2}{2}\right)^2 + u_{worm0}^2 + \left(\frac{E_{wgear}/2}{2}\right)^2 \tag{10}$$

3.4.4 Uncertainty of double-flank rolling test execution (u_{df})

This term of uncertainty must include any influence due to the development of the two-flank rolling test, which has not been previously covered in any other term. Equation (*11*) show s the uncertainty expression divided into

the uncertainty associated with the small displacements of the secondary carriage (u_{dfd}) and the uncertainty of the rest of the parameters of the test execution (u_{dfp}).

In the first component, the uncertainty due to the laser interferometer used in the numerical compensation (u_{lix1}), the uncertainty of the accuracy of the length gauge (u_{lgx1}) and the uncertainty associated with the secondary carriage displacement compensation (u_{dfdc}) have been considered. All of them use the same sensitivity coefficient (c_{cdFi}) related to the x-axis movement (equation *12*). Finally, the second term is composed of the uncertainty due to the rotation speed during test (u_{rs}), the uncertainty due to the force exerted by the elastic system (u_{es}) and of any other uncertainty that would be taken into account (u_{others}). This last term was considered negligible since the recommendations of the standards were followed [5].

$$u_{df}^2 = u_{dfd}^2 + u_{dfp}^2 = \left(u_{lix1}^2 + u_{lgx1}^2 + u_{dfdc}^2\right) + \left(u_{rs}^2 + u_{es}^2 + u_{others}^2\right) \quad (11)$$

$$u_{df}^2 = c_{cdFi}^2 \left[\left(\frac{E_{lix1}}{\sqrt{3}}\right)^2 + \left(\frac{E_{lgx1}}{\sqrt{3}}\right)^2 + \left(\frac{E_{XX1}/2}{\sqrt{3}}\right)^2\right] + \left(u_{rs}^2 + u_{es}^2 + u_{others}^2\right) \quad (12)$$

3.5 Expanded uncertainty of F_i'' parameter

Table 7 summarizes the values of the uncertainty components for the calculation of the combined standard uncertainty of the total radial composite deviation $u_c\ (F_i'')$. It also includes their evaluation and distribution type, their component of individual standard uncertainty, their sensitivity coefficients, their degrees of freedom (v_{eff}) as well as their percentage contribution to total uncertainty. Finally, the expanded uncertainty of the total radial composite deviation of the measurement $U_{95}\ (F_i'')$ has been calculated according to equation (*3*), applying a coverage factor *k=2* established from the effective degrees of freedom by Welch-Satterthwaite formula [16]. Its value is equal to 5.6 µm with a confidence interval of 95%, for the entire measurement volume. It is observed that the greatest of the contributions is concentrated in the worm gear mounting with a percentage of 82.99% and the rest could practically be assigned to the displacement of the main horizontal carriage, with a percentage of 16.93%.

Table 7 *Summary of the uncertainty budget of F_i'' parameter for the entire measurement volume*

$u(x_i)$		Eval. / Distr.	$u(x_i)$ (µm)	c_i	$u_i(F_i'')=c_i \cdot u(x_i)$ (µm)	v_{eff}	$\frac{u(x_i)^2}{u_c(F_i'')^2}$ (%)
u_0			**0.08**	**1**	**0.08**	**$7.7 \cdot 10^6$**	**0.09**
	u_{0cg}		0.004	1	0.004	488	0
	u_{0cgw}		0.005	0.5	0.003	863	0
	u_{CMM}	B	0.333	0.013	0.004	∞	0
	u_{Scgw}	A	0.063	0.013	0.001	9	0
	$u_{\Delta t}$	B/Rect	0.198	0.013	0.003	∞	0
	u_{0cgwg}		0.005	0.5	0.002	129	0
	u_{CMM}	B	0.333	0.013	0.004	∞	0
	u_{Scgwg}	A	0.095	0.013	0.001	9	0
	$u_{\Delta t}$	B/Rect	0.126	0.013	0.001	∞	0
	u_{0encx}	B/Rect	1.732	0.013	0.023	∞	0.01
	u_{0lgx1}		0.008	1	0.008	4290	0
	u_{lgx1}	B/Rect	0.577	0.013	0.008	∞	0
	u_{rsc}	A	0.127	0.013	0.002	9	0

	u_{ocgz}		0.016	0.5	0.008	836	0
	u_{CMM}	B	0.333	0.040	0.013	∞	0
	u_{Scgw}	A	0.063	0.040	0.003	9	0
	$u_{\Delta t}$	B/Rect	0.198	0.040	0.008	∞	0
	u_{0cncz}	B/Rect	1.732	0.040	0.069	∞	0.06
	u_{0p}		0.034	1	0.034	∞	0.01
	u_{pr}	B/Rect	0.850	0.039	0.033	∞	0.01
	u_{pdg}	B/Rect	0.213	0.039	0.008	∞	0
u_{dis}			**1.16**	**1**	**1.16**	∞	**16.92**
	u_{cd}		1.10	1	1.10	∞	15.44
	u_{lix}	B/Rect	0.116	0.013	0.002	∞	0
	u_{encx}	B/Rect	1.732	0.013	0.023	∞	0.01
	u_{cdb}		1.100	1	1,099		15.43
	u_{cdc}	B/Rect	0.924	0.013	0.010	∞	0
	u_{cdEZX}	B/Rect	16.166	0.040	0.647	∞	5.35
	u_{cdEBX}	B/Rect	21.939	0.040	0.878	∞	9.80
	u_{cdEAX}	B/Rect	3.753	0.039	0.146	∞	0.28
	u_{h}		0.34	1	0.34	∞	1.49
	u_{liz}	B/Rect	0.043	0.040	0.002	∞	0
	u_{encz}	B/Rect	1.732	0.040	0.069	∞	0.06
	u_{hb}		0.335	1	0.335		1.43
	u_{hc}	B/Rect	1.241	0.040	0.050	∞	0.03
	u_{hEBZ}	B/Rect	2.598	0.040	0.104	∞	0.14
	u_{hEAZ}	B/Rect	8.083	0.039	0.315	∞	1.26
	u_{hEXZ}	B/Rect	0.000	0.013	0.000	∞	0.00
u_{gear}			**2.56**	**1**	**2.56**	∞	**82.99**
	u_{worm}	B/Gauss	0.23	1	0.23	∞	0.67
	u_{worm0}		0	1	0	∞	0
	u_{wgear}	B/Gauss	2.55	1	2.55	∞	82.32
u_{df}			**0.008**	**1**	**0.008**	∞	**0**
	u_{dfd}		0.008	1	0.008	∞	0
	u_{lix1}	B/Rect	0.116	0.013	0.001	∞	0
	u_{lgx1}	B/Rect	0.577	0.013	0.007	∞	0
	u_{dfc}	B/Rect	0.116	0.013	0.001	∞	0
	u_{dfp}		0	1	0	∞	0
u_c (F_i'')					**2.81**		**100**
U_{95} (F_i'', k=2)					**5.6**		

3.6 Expanded uncertainty of F_r'' and f_i'' parameters

The accuracy grade of a gear by rolling test is determined by the worst accuracy grade obtained from any of its three parameters (F_i'', F_r'', f_i''). This means that it is also necessary to know the expanded uncertainty of F_r'' and f_i'' parameters. They can be estimated applying equation (*3*), because of being subject to the same sources of error. Nevertheless, different values of repeatability in the assembly of the gears (Table 5) as well as different sensitivity coefficients (Table 6) have to be applied to consider the contribution for each uncertainty source depending on how it influences each measurand.

Table 8 summarizes the values of the uncertainty components for the calculation of the combined standard uncertainty of the runout in the radial composite test u_c (F_r''). Its expanded uncertainty U_{95} (F_r'') with coverage factor $k=2$ is equal to 5.0 μm for the entire measurement volume. The greatest of the contributions is concentrated in the worm gear mounting, with a percentage of 95.92%, because this parameter by definition represents the eccentricity of the gear hobbing.

Table 8 *Summary of the uncertainty budget of F_r'' parameter for the entire measurement volume*

$u(x_i)$		$u_i(F_r'')=c_i \cdot u(x_i)$ (μm)	v_{eff}	$\frac{u(x_i)^2}{u_c(F_r'')^2}$ (%)
u_0		**0.06**	**$1.2 \cdot 10^6$**	**0.06**
u_{dis}		**0.48**	∞	**3.75**
	u_{cd}	0.38	∞	2.31
	u_h	0.30	∞	1.44
u_{gear}		**2.45**	∞	**96.19**
	u_{worm}	0.13	∞	0.27
	u_{wgear}	2.45	∞	95.92
u_{sf}		**0.01**	∞	**0**
$u_c(F_r'')$		**2.50**		**100**
$U_{95}(F_r'', k=2)$		**5.0**		

Table 9 *Summary of the uncertainty budget of f_i'' parameter for the entire measurement volume*

$u(x_i)$		$u_i(f_i'')=c_i \cdot u(x_i)$ (μm)	v_{eff}	$\frac{u(x_i)^2}{u_c(f_i'')^2}$ (%)
u_0		**0.07**	**$3.1 \cdot 10^6$**	**0.47**
u_{dis}		**0.90**	∞	**76.85**
	u_{cd}	0.88	∞	73.05
	u_{lix}	0.002	∞	0
	u_{encx}	0.033	∞	0.10
	u_{cdc}	0.018	∞	0.03
	u_{cdEZX}	0.52	∞	25.71
	u_{cdEBX}	0.70	∞	46.59
	u_{cdEAX}	0.08	∞	0.61
	u_h	0.20	∞	3.78
u_{gear}		**0.49**	∞	**22.67**
	u_{worm}	0.28	∞	7.46
	u_{wgear}	0.40	∞	15.21
u_{sf}		**0.01**	∞	**0.01**
$u_c(f_i'')$		***1.02***		**100**
$U_{95}(f_i'', k=2)$		**2.0**		

Table 9 summarizes the values of the uncertainty components for the calculation of the combined standard uncertainty of the tooth-to-tooth radial composite deviation $u_c(f_i'')$. Its expanded uncertainty $U_{95}(f_i'')$ with coverage factor $k=2$ is equal to 2.0 µm for the entire measurement volume. In this case, the highest contribution comes from the displacement of the main horizontal carriage, with a percentage of 76.85%, and not from the worm gear mounting because, theoretically, f_i'' parameter is a eccentricity-free parameter.

4. Optimization of uncertainty budget

The estimated uncertainty values show that it is difficult to establish the accuracy grade of a worm gear when the rolling parameters values (F_i'', F_r'', f_i'') are close to the limit between two grades (table 3), especially in the verification of high quality gears (accuracy grade below 6). The advantage of the uncertainty budget is that it

allows knowing the influence of each error source individually. In this way, it is possible to focus on the main error sources to reduce the uncertainty of the measurement process.

In this case of study, the worm gear mounting and the displacement of the horizontal carriage to its nominal test position were detected as the greatest error sources. A new uncertainty estimation, more adjusted to reality, could be estimated. On one hand, a new clamping system could be evaluated to minimize the eccentricity of the worm gears. On the other hand, we could consider the displacements reduced to the usual working area (up to 200 mm in the x-axis and up to 50 mm in the z-axis) minimizing significantly the errors of (u_{cdb}) and (u_{hb}) uncertainty terms (Table 4).

In this section, new optimized uncertainty budgets of F_i'', F_r'' and f_i''parameters are proposed (Table 10, Table 11, Table 12). The worm gear mounting repeatability values of the f_i'' parameter (eccentricity-free) have been considered, as well as a measurement volume for worm gears up to 400 mm in diameter. In addition, these new uncertainty budgets for F_i'', F_r'' and f_i''parameters show different contributions in percentage and allow us to define a new improvement plan for the uncertainty components. As an example, linear guides could be readjusted to try to eliminate part of the pitch error (E_{BX}) or even, failing that, to replace those guides by greater accuracy ones.

Table 10 *Summary of the optimized uncertainty budget of F_i'' parameter*

$u(x_i)$		$u_i(F_i'')=c_i \cdot u(x_i)$ (μm)	$\frac{u(x_i)^2}{u_c(F_i'')^2}$ (%)
u_0		**0.08**	**1.25**
u_{dis}		**0.55**	**58.35**
	u_{cd}	0.55	56.60
	u_{lix}	0.002	0
	u_{encx}	0.023	0.10
	u_{cdc}	0.010	0.02
	u_{cdEZX}	0.19	7.21
	u_{cdEBX}	0.49	46.58
	u_{cdEAX}	0.11	2.42
	u_h	0.10	1.75
u_{gear}		**0.46**	**40.38**
	u_{worm}	0.23	10.03
	u_{wgear}	0.40	30.35
u_{sf}		**0.01**	**0.02**
$u_c(F_i'')$		**0.73**	**100**
$U_{95}(F_i'', k=2)$		**1.5**	

Table 11 *Summary of the optimized uncertainty budget of F_r'' parameter*

$u(x_i)$		$u_i(F_r'')=c_i \cdot u(x_i)$ (μm)	$\frac{u(x_i)^2}{u_c(F_r'')^2}$ (%)
u_0		**0.06**	**1.58**
u_{dis}		**0.22**	**20.89**
	u_{cd}	0.21	19.32
	u_h	0.06	1.58
u_{gear}		**0.42**	**77.49**
	u_{worm}	0.13	7.40

	u_{wgear}	0.40	70.08
u_{sf}		**0.01**	**0.04**
$u_c (F_r'')$		**0.48**	**100**
$U_{95} (F_r'', k=2)$		**1.0**	

Table 12 *Summary of the optimized uncertainty budget of f_i'' parameter*

$u(x_i)$		$u_i(f_i'')=c_i \cdot u(x_i)$ (µm)	$\frac{u(x_i)^2}{u_c(f_i'')^2}$ (%)
u_0		**0.07**	**1.12**
u_{dis}		**0.44**	**44.54**
	u_{cd}	0.44	43.42
	u_{lix}	0.002	0
	u_{encx}	0.033	0.25
	u_{cdc}	0.016	0.06
	u_{cdEZX}	0.16	5.83
	u_{cdEBX}	0.40	36.46
	u_{cdEAX}	0.06	0.82
	u_h	0.07	1.12
u_{gear}		**0.49**	**54.32**
	u_{worm}	0.28	17.86
	u_{wgear}	0.40	36.46
u_{sf}		**0.01**	**0.02**
$u_c (f_i'')$		**0.66**	**100**
$U_{95} (f_i'', k=2)$		**1.3**	

Table 13 compares the original estimated values of the expanded uncertainty with the optimized ones, revealing that a significant reduction in the uncertainty of all the parameters could be possible.

Table 13 *Comparison between original and optimized expanded uncertainty*

	F_i'' (µm)	F_r'' (µm)	f_i'' (µm)
U_{95}	5.6	5.0	2.0
U_{95opt}	1.5	1.0	1.3
Reduction	73%	80%	35%

5. Conclusions

The uncertainty budget method, according to GUM guidelines, allows knowing which are the main sources of error in a measurement process. In this work, a general expression has been proposed to estimate the expanded uncertainty of double-flank gear rolling tests. A case study of a double-flank gear rolling tester for worm gear has been used to present the expression developed. The measurement uncertainty has been calculated from experimental data of the tester repeatability.

Despite the large number of error sources that are combined in this type of tests, the results show that it is possible to break down each of them into elementary terms. In this way, we were able to determine with certain precision what is their individual contribution to the global measurement uncertainty. In particular, it could be highlighted in the case study that: (i) the lack of repeatability in the worm gear clamping is presented as the main

error source directly affecting the F_i'' and F_r'' parameters; (ii) the geometric errors in the carriages' displacements, mainly due to the backlash in linear guides, meant the greatest influence on the f_i'' parameter; (iii) the errors in the initial calibration have hardly any influence; and (iv) the uncertainty due to the test execution is considered negligible because the parameters recommended by the standards (rotation speed and elastic system force) have been respected.

Moreover, after the first analysis, an optimization of the uncertainty estimation has been proposed in a second iteration. On one hand, the measurement uncertainty has been adjusted by reducing the displacements to a more realistic working area, and on the other hand, the uncertainty of a worm gear clamping of higher quality has been considered. In this manner, the estimation of measurement uncertainty can significantly be minimized at the same time that new sensitive points of improvement can be established through the new uncertainty budget. This means that we can act on certain sources of error to increase the accuracy of a tester, being able to verify gears of better quality. However, this could involve recalibrating the equipment after adjusting some mechanical components, modifying the design of certain elements and/or even replacing the measuring instruments with others of higher accuracy.

In spite of the lack of traceability at NMIs and DIs for worm and worm gear measurements, the method and guidelines developed in this paper allow establishing the accuracy of any double-flank rolling gear testers or gear measuring machines based on its functioning principles. It can also help to understand the behaviour of this type of measurement instrument so widespread in the industry. In this manner, the main sources of uncertainty can be determined to improve actual gear measurement capacities. Furthermore, this method could be applied to the development of new verification equipment because critical design points can be easily defined.

Acknowledgements

This work has been possible thanks to the technical and human support of Echeverría Construcciones Mecánicas S.A.

References

[1] Goch G. Gear metrology. CIRP Ann - Manuf Technol 2003;52:659–95. doi:10.1016/S0007-8506(07)60209-1.

[2] Lawson E. The Basics of Gear Metrology and Terminology Part I. Gear Technol 1998;15:41–50.

[3] ISO 1328-1:2013 Cylindrical gears - ISO system of accuracy - Part 1: Definitions and allowable values of deviations relevant to corresponding flanks of gear teeth. 2013.

[4] ISO 1328-2:1997 Cylindrical gears - ISO system of accuracy - Part 2: Definitions and allowable values of deviations relevant to radial composite deviations and runout information. 1997.

[5] VDI/VDE 2608 Tangential composite and radial composite inspection of cylindrical gears, bevel gears, worm and worm wheels. 2001.

[6] Pueo M, Santolaria J, Acero R, Gracia A. A review of tangential composite and radial composite gear inspection. Precis Eng 2017;50:522–37. doi:10.1016/j.precisioneng.2017.05.007.

[7] Michalec GW. Precision Gearing: Theory and Practice. Wiley; 1966.

[8] Thoen RL. Calibration of Two-Flank Roll Testers. Gear Technol 2008;25:58–60.

[9] Pueo Arteta M, Santolaria Mazo J, Acero Cacho R, Aso Arjol G. Double flank roll testing machines intercomparison for worm and worm gear. Procedia Eng., vol. 63, 2013. doi:10.1016/j.proeng.2013.08.231.

[10] ISO 18653:2003 Gears - Evaluation of instruments for the measurement of individual gears. 2003.

[11] ISO/TR 10064-5:2005 Code of inspection practice - Part 5: Recommendations relative to evaluation of gear measuring instruments. 2005.

[12] AGMA 931-A2 Calibration of Gear Measuring Instruments and Their Application to the Inspection of Product Gears. 2002.

[13] ANSI/AGMA 2116-A05 Evaluation of Double Flank Testers for Radial Composite Measurement of Gears. 2005.

[14] AGMA 935-A05 Recommendations Relative to the Evaluation of Radial Composite Gear Double Flank Testers. 2005.

[15] Frazer RC, Wilson SJ. Implementing ISO 18653 - Gears: Evaluation of Instruments for Measurement of Individual Gears. Gear Technol 2010;27:38–47.

[16] Joint Committee for Guides in Metrology. JCGM 100:2008 Evaluation of measurement data: Guide to the expression of uncertainty in measurement (GUM 1995 with minor corrections). 2008.

[17] Frazer RC. Measurement Uncertainty in Gear Metrology. Ph.D. dissertation. Newcastle University, UK, 2007.

[18] Reiter E, Eberle F. Practical Considerations for the Use of Double-Flank Testing for the Manufacturing Control of Gearing - Part I. Gear Technol 2014;31:44–51.

[19] Tang J, Shi Z. Repeatability test of in-line gear measuring machine. 7th Int. Symp. Precis. Eng. Meas. Instrum., vol. 8321, 2011, p. 832115. doi:10.1117/12.903984.

[20] Tang J, Jia J, Fang Z, Shi Z. Development of a gear measuring device using DFRP method. Precis Eng 2016;45:153–9. doi:10.1016/j.precisioneng.2016.02.006.

[21] Tang J, Zhang Y, Shi Z. Radial and tangential error analysis of double-flank gear measurement. Precis Eng 2018;51:552–63. doi:10.1016/j.precisioneng.2017.10.011.

[22] ISO 14253-2:2011 Geometrical product specifications (GPS) - Inspection by measurement of workpieces and measuring equipment - Part 2: Guidance for the estimation of uncertainty in GPS measurement, in calibration of measuring equipment and in product veri. 2011.

[23] Munro RG. Effect of Geometrical Errors on the Transmission of Motion between Gears. Proc Inst Mech Eng 1969;184:79–84.

[24] Smith RE. What Single Flank Measurement Can Do For You. AGMA Fall Tech. Meet. 84 FTM 2, Washington, DC: 1984, p. 1–12.

[25] Knapp W. Measurement Uncertainty and Machine Tool Testing. CIRP Ann - Manuf Technol 2002;51:459–62. doi:10.1016/S0007-8506(07)61560-1.

[26] Pueo M, Santolaria J, Acero R, Cajal C, Gracia A. Universal Roll Testing Machine for Worm and Worm Gear. Procedia Eng., vol. 132, 2015, p. 848–55. doi:10.1016/j.proeng.2015.12.569.

[27] AGMA 915-1-A02 Inspection Practices - Part 1: Cylindrical Gears - Tangential Measurements. 2002.

[28] AGMA 915-2-A05 Inspection Practices - Part 2: Cylindrical Gears - Radial Measurements. 2005.

[29] ANSI/AGMA. ANSI/AGMA 2111-A98 Cylindrical wormgearing tolerance and inspection methods. 1998.

[30] Schwenke H, Knapp W, Haitjema H, Weckenmann A, Schmitt R, Delbressine F. Geometric error measurement and compensation of machines—An update. CIRP Ann - Manuf Technol 2008;57:660–75. doi:10.1016/j.cirp.2008.09.008.

[31] Bicker R, Frazer RC, Wehrneyer D. Verifying position errors in CNC gear measuring instruments using a laser interferometer with dynamic data capture software. Laser Metrol. Mach. Perform. V, vol. 34, 2001, p. 345–54.

[32] Frazer RC, Hu J. Methods of testing calibration equipment in the UK's national gear metrology laboratory. Laser Metrol. Mach. Perform. III, vol. 16, 1997, p. 231–41.

[33] ISO 230-1:2012 Test code for machine tools - Part 1: Geometric accuracy of machines operating under no-load or quasi-static conditions. 2012.

[34] ISO 230-2:2014 Test code for machine tools - Part 2: Determination of accuracy and repeatability of positioning of numerically controlled axes. 2014.

[35] Pueo M, Santolaria J, Acero R, Aguado S, Gracia A. A new calibration guideline for worm and worm-gear rolling testers. Procedia Manuf 2017;13:601–7. doi:10.1016/j.promfg.2017.09.119.